



## Review Article

# Distribution of relaxation times: Foundations, methods, diagnostics, and prognosis for electrochemical systems

Zilong Wang<sup>1</sup>, Yuhao Wang<sup>1</sup> and Francesco Ciucci<sup>1,2,3</sup>

The distribution of relaxation times (DRT) has become an indispensable technique for interpreting electrochemical impedance spectroscopy. This review traces the evolution of DRT from a powerful deconvolution tool for gaining mechanistic insights into a predictive engine for diagnostics and state estimation in fields such as batteries and fuel cells. The technique's intuitive appeal is challenged by its mathematically ill-posed nature, creating a "credibility gap" where subjective choices can yield misleading artifacts. Recent methodological advances in Bayesian and entropy-based frameworks provide greater robustness and uncertainty quantification. The path forward requires establishing a comprehensive analytical ecosystem built on community standards, benchmark datasets, and transparent reporting. This current opinion urges the community to embrace rigor and transform DRT from a specialized, expert-level tool into a reliable and reproducible cornerstone of electrochemical analysis.

**Addresses**

<sup>1</sup> Department of Mechanical and Aerospace Engineering, The Hong Kong University of Science and Technology, Clear Water Bay, Kowloon, Hong Kong S.A.R., China

<sup>2</sup> Chair of Electrode Design for Electrochemical Energy Systems, University of Bayreuth, Weiherstraße 26, 95448 Bayreuth, Bavaria, Germany

<sup>3</sup> Bavarian Center for Battery Technology (BayBatt), University of Bayreuth, Universitätsstraße 30, 95447 Bayreuth, Germany

Corresponding authors: Wang, Zilong ([zl.wang@connect.ust.hk](mailto:zl.wang@connect.ust.hk)); Ciucci, Francesco ([francesco.ciucci@ust.hk](mailto:francesco.ciucci@ust.hk)), ([francesco.ciucci@uni-bayreuth.de](mailto:francesco.ciucci@uni-bayreuth.de)); Wang, Yuhao ([yuhao.wang@connect.ust.hk](mailto:yuhao.wang@connect.ust.hk))

kinetics and transport [1]. Equivalent-circuit fits are often nonunique, as distinct circuits can fit the same data, and elements may lack a clear physical meaning [2]. The distribution of relaxation times (DRT) offers an alternative by transforming  $Z(\omega)$  into a time-constant domain representation  $\gamma(\log \tau)$  [3]. In an ideal DRT, distinct processes appear as separate peaks as a function  $\log \tau$ , where the peak position indicates the characteristic timescale, and the peak area, integrated over  $\log \tau$ , is proportional to that process's contribution to the total polarization resistance [4]. Because the DRT is agnostic to circuit topology, it yields a compact fingerprint of system dynamics. Its interpretative and visualization power increases when spectra are collected under controlled variations (*e.g.* temperature, state of charge [SOC], and partial pressure), letting correlated peak shifts be mapped to specific mechanisms through coupling with prior work or companion experiments (*e.g.* thermally activated processes shift to shorter times with increasing temperature [5]).

Despite its intuitive appeal, DRT is not a push-button method. It rests on the basic assumption that a linear, time-invariant electrochemical system responds as a superposition of elementary relaxations. Under this assumption, the impedance and the DRT are related by a Fredholm integral equation of the first kind, which is written as follows[3]

$$Z(\omega) = R_{\infty} + i\omega L_0 + \frac{1}{i\omega C_0} + \int_{-\infty}^{+\infty} \frac{\gamma(\log \tau)}{1 + i\omega\tau} d \log \tau \quad (1)$$

where  $\omega$  is an angular frequency ( $\omega = 2\pi f$  with  $f$  being a frequency),  $R_{\infty}$ ,  $C_0$ , and  $L_0$  are the series resistance (*e.g.* electrolyte resistance), capacitance, and inductance, respectively, and  $i$  is the imaginary unit. The forward DRT operator is linear in that linear combinations of DRTs map to linear combinations of impedances. Although the forward map is functional and, thus, nonparametric, in practice  $\gamma(\log \tau)$ , it is most often (but not always) approximated through a fixed and finite representation, namely a basis expansion in  $\log \tau$  [6].

Recovering  $\gamma(\log \tau)$  from discrete, noisy measurements of  $Z(\omega)$  is an ill-posed inverse problem ( $\frac{1}{1+i\omega\tau}$  is smoother), and minor experimental errors can cause large, oscillatory artifacts, resulting in DRT estimates that are not

Current Opinion in Electrochemistry 2026, 55:101789

This review comes from a themed issue on **Electrochemical Impedance Spectroscopy (EIS) (2025)**

Edited by **Mark E. Orazem** and **Vincent Vivier**

For complete overview about the section, refer [Electrochemical Impedance Spectroscopy \(EIS\) \(2025\)](#)

Available online 26 November 2025

<https://doi.org/10.1016/j.coelec.2025.101789>

2451-9103/© 2026 The Authors. Published by Elsevier B.V. This is an open access article under the CC BY license (<http://creativecommons.org/licenses/by/4.0/>).

**Introduction**

Electrochemical impedance spectroscopy (EIS) is a mainstay in electrochemistry for probing charge transfer

physically plausible. Stabilization requires regularization, that is, augmenting the data-fit objective with constraints (*e.g.* smoothness, non-negativity, and sparsity) that suppress noise amplification while preserving resolvable structure. Open-source tools have accelerated the adoption of DRT across various electrochemical applications, including batteries and fuel cells, as well as corrosion, semiconductors, and bioimpedance [7]. This rapid interest, however, has at times outpaced a full appreciation of the method's mathematical details, strengths, and limitations. As the goal is to obtain a DRT that is both stable and interpretable, the resulting perception of simplicity carries a risk of overinterpretation, particularly because practical analysis introduces user choices that trade off data fidelity against solution smoothness. A critical, standard-based practice benchmarked against separate experimentation is therefore essential. This article highlights recent methodological advances that reduce subjectivity and improve robustness, and it surveys the new classes of applications enabled by these more reliable approaches. To orient the reader, [Figure 1](#) summarizes recent developments of DRT's methodological foundations, core applications in electrochemical energy systems, and emerging technologies, providing a visual roadmap to the following sections.

### From impedance to DRT: Mathematical framework and the ill-posed inverse problem

Eq. (1) defines the forward map from the DRT to the impedance. Under standard regularity conditions, each admissible  $\gamma(\log \tau)$  yields a unique impedance  $Z(\omega)$ . Formally, one may also write the following inverse representation that expresses (under several assumptions)  $\gamma(\log \tau)$  in terms of an analytic continuation of  $Z(\omega)$  into the complex plane [8,9]<sup>1</sup> as follows:

$$\gamma(\log \tau) = -\frac{1}{\pi} \Im \left[ Z\left(\frac{i}{\tau}\right) - Z\left(-\frac{i}{\tau}\right) \right] \quad (2)$$

where the latter equation has close connections to the inverse of the Stieltjes transform [10]. In practice, this expression requires the recovered impedance to be an analytic function over the complex plane, whereas EIS measurements provide noisy  $Z(\omega)$  data only at discrete frequencies over the positive real axis ( $\omega > 0$ ). Accordingly, to estimate the DRT one either (i) posits a representation for  $\gamma(\log \tau)$  and fits it *via* Eq. (1) or (ii) regresses  $Z(\omega)$  using an analytic model (*e.g.* an equivalent circuit) and then recovers  $\gamma(\log \tau)$  using Eq. (2). This distinction is essential as the DRT is not merely a sum of RC-Voigt-like elements; it is a specific form of the Stieltjes transform between the frequency and time-constant domains [10], yet Eq. (2) is not universally applicable and must be interpreted in the sense of distributions at simple RC poles; in fact, if Eq. (2) is used naively,  $\gamma(\log \tau)$  vanishes away from the pole and is undefined at the pole itself. Likewise, for

unbounded elements that represent semi-infinite processes, the DRT diverges and should be treated in an *ad hoc* fashion and in the sense of generalized functions. As an illustration, the open-circuit, finite-length, blocking 1D transmission-line model cannot be used in a simple vanilla sense within the context of the DRT. The impedance of [11]

$$Z(\omega) = R \frac{\coth \sqrt{i\omega\tau_0}}{\sqrt{i\omega\tau_0}} \quad (3)$$

which is unbounded and converges to infinity, yet even a seemingly intractable element like that given in Eq. (3) admits a DRT. For instance, we can rewrite using Mittag-Leffler expansion as follows:

$$Z(\omega) = \frac{R}{i\omega\tau_0} + 2R \sum_{n=1}^{\infty} \frac{1}{1 + i\omega \frac{\tau_0}{(n\pi)^2}} \quad (4)$$

where upon subtraction of the capacitive terms, the characteristic times  $\tau_n = \frac{\tau_0}{(n\pi)^2}$  are the locations of the poles of  $Z(\omega)$ .

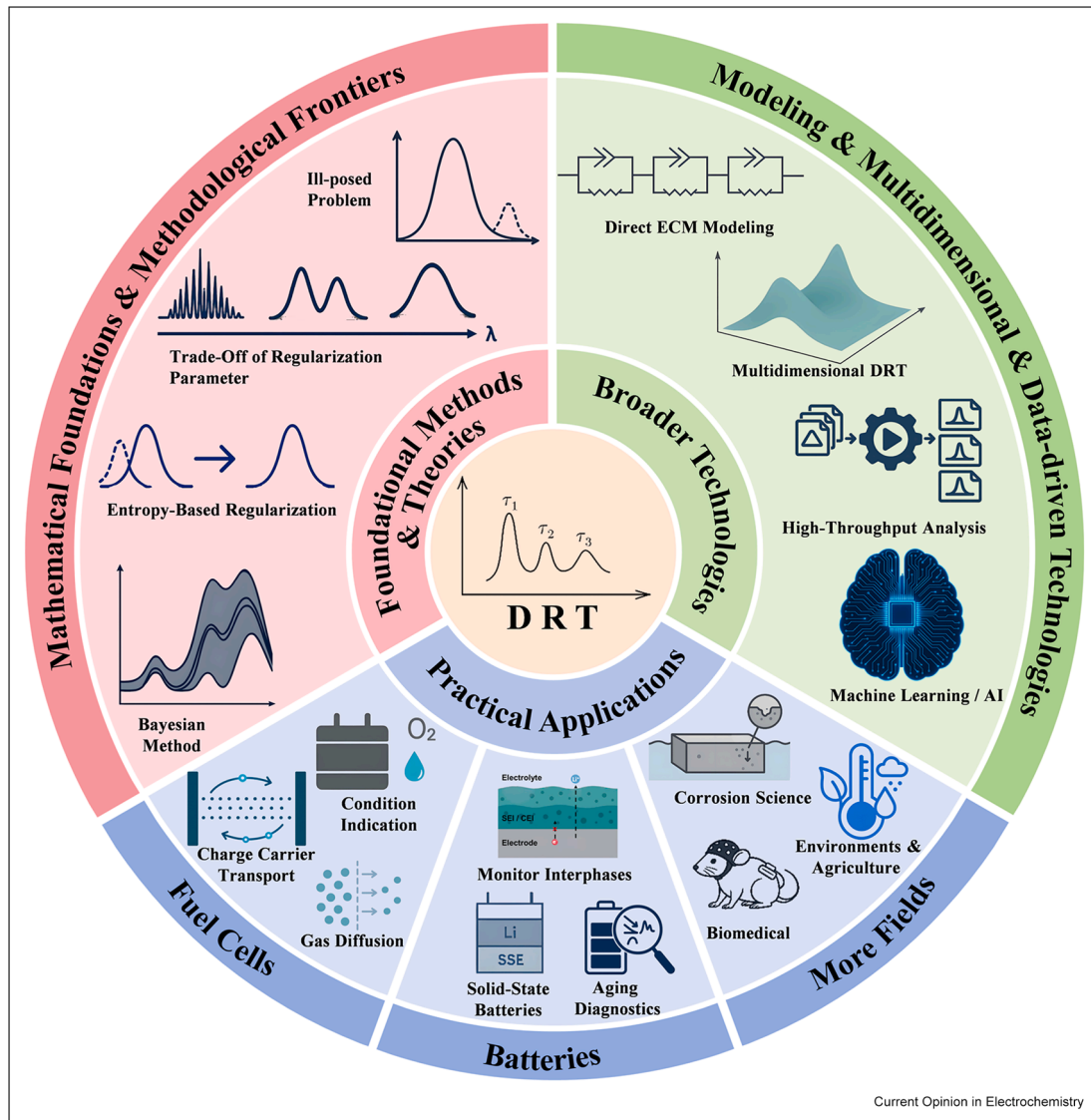
In practice, DRT deconvolution is implemented *via* surrogate models which can be (i) nonparametric, including Gaussian-process priors or nonparametric Bayesian mixtures (*e.g.* Dirichlet-process mixtures); (ii) parametric, featuring for instance structured peak families or neural networks; or (iii) semiparametric, that is, hybrids that couple a parametric core with a nonparametric component [12,13]. Physical interpretation remains delicate as identifiability limits persist; robust peak-to-mechanism assignments require support *via* complementary measurements, prior work, or mechanistic modeling.

### Methodological frontiers toward robust and trustworthy DRT analysis

Inverting through Eq. (1) from noisy data is ill-posed because even tiny perturbations in data can cause large, oscillatory changes in a finite representation of data, leading to many different DRTs that fit the data within experimental errors [14]. Regularization restores stability by minimizing a weighted sum of data misfit and a penalty on the roughness or complexity of  $\gamma(\log \tau)$ . Tikhonov (ridge) remains widely used, typically penalizing the 0th, first, or second derivative to favor DRT simplicity or smoothness, with the regularization parameter  $\lambda$  governing the resolution–stability trade-off. Small  $\lambda$  yields high resolution but gives noise-amplifying, peak-rich solutions. In contrast, large  $\lambda$  suppresses noise at the risk of over-smoothing and peak merging ([Figure 2\(a\)](#)) [3,6]. The regularization level  $\lambda$  is typically chosen using methods like the L-curve, generalized cross-validation (GCV), or the discrepancy principle. While these methods are practical, they are not universally optimal. Furthermore, before adjusting  $\lambda$ , it is advisable to perform Kramers–Kronig (KK)/Hilbert consistency checks on the raw impedance data to assess random and systematic errors. Ignoring this step can lead to contamination from drift, lead inductance,

<sup>1</sup> Extensions to this formula including taking into account poles in the impedance are also available.

Figure 1



A landscape of DRT's recent progress: foundational methods, theories, practical applications, and broader technologies. DRT, distribution of relaxation times.

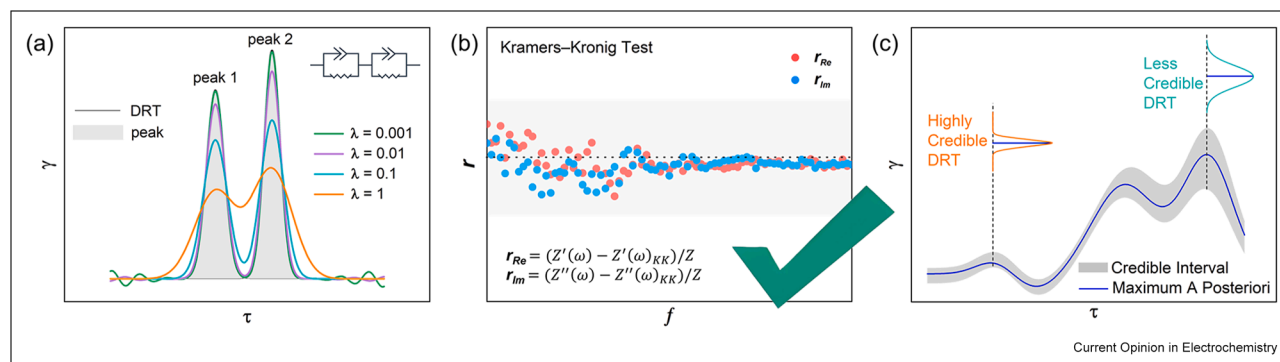
or nonlinearity, which may bias the DRT and distort the inversion results (see Figure 2(b)). For data consistent with KK/Hilbert relations, adaptive and hybrid techniques such as hierarchical or Bayesian  $\lambda$  selection, entropy penalties, and scale-dependent smoothing can enhance stability while maintaining the resolution of peaks in complex systems.

A major advance is the adoption of Bayesian methods, which move from seeking a single best-fit DRT to estimating a full posterior over admissible DRTs (Figure 2(c)) [15–17]. Treating  $\gamma(\log \tau)$  as a random process and incorporating prior knowledge (*e.g.* nonnegativity and smoothness), Bayes' theorem yields credible bands that

widen appropriately with noise and helps prevent over-interpretation of artifacts. Hierarchical models can learn the regularization level from the data, mitigating subjectivity. Entropy-based regularization offers an alternative to smoothness penalties by favoring the maximum-entropy distribution consistent with the data; this often suppresses unphysical peaks and avoids undue peak broadening observed with ridge regression [18] (Table 1). These frameworks also support uncertainty quantification and joint inversion of multiple spectra.

Recent work distinguishes two objectives in DRT analysis, namely (i) regression, which estimates the continuous amplitude of the DRT across time scales and (ii) process

Figure 2



Mathematical foundations and methodological frontiers. (a) Distributions obtained by the DRT analysis with a variation of different  $\lambda$  values. (b) An example of residual results from Kramers–Kronig (KK) tests. (c) An example of a Bayesian DRT analysis result. DRT, distribution of relaxation times.

Table 1

## Comparison of different regularization methods.

Method	Underlying principles	Key advantages	Key limitations
Tikhonov regularization	Minimizes squared error + roughness penalty	Simple, computationally fast, and widely available	Highly sensitive to subjective choice of regularization parameter ( $\lambda$ ); prone to artifacts
Bayesian/hierarchical Bayesian	Computes a posterior probability distribution of possible DRTs	Provides quantitative uncertainty quantification (credible intervals); can be self-tuning	Computationally more intensive than simple regularization
Entropy-based regularization	Minimizes squared error + entropy penalty (favors smoothness)	Effectively suppresses spurious peaks and noise-induced artifacts; high accuracy	Can be computationally intensive; newer and less widely implemented
Dual-regression classification	Unifies regression (magnitude) and classification (process identification) tasks	Provides novel metrics for accuracy; enables autonomous model selection	A conceptual framework with emerging algorithms; still under active development

DRT, distribution of relaxation times.

identification, a quasi-classification task that infers the number and locations (in  $\log \tau$ ) of discrete processes. The latter can be pursued sequentially (first estimating  $\gamma(\log \tau)$  via Eq. (1), then detecting peaks) or jointly with models that infer a finite, data-determined set of components and their amplitudes (e.g. Bayesian mixtures) without prespecifying the component count. Making process identification explicit enables autonomous model selection and metrics that assess both the quality of fitting and the correctness of process detection. These approaches are promising but remain at an early stage [14,19].

Machine learning models, including Gaussian processes and neural networks, tackle the ill-posed DRT inversion by embedding regularization in the prior and architecture (e.g. kernel choice, weight decay, and smoothness/monotonicity constraints), which stabilizes the estimate

[20]. They perform best when constrained by physics (KK consistency, non-negativity, and causality) and validated against synthetic and experimental ground truth with calibrated uncertainty.

### From interpreting spectra to predicting failure: DRTs expanding role

Recent advances in DRT deconvolution have broadened the scope of DRT, shifting it from primarily interpretive analysis to a practical basis for predictive diagnostics in operational systems.

### Core applications: achieving deeper mechanistic insights

In the field of ionic materials, encompassing batteries and fuel cells, DRT is routinely used to separate impedance

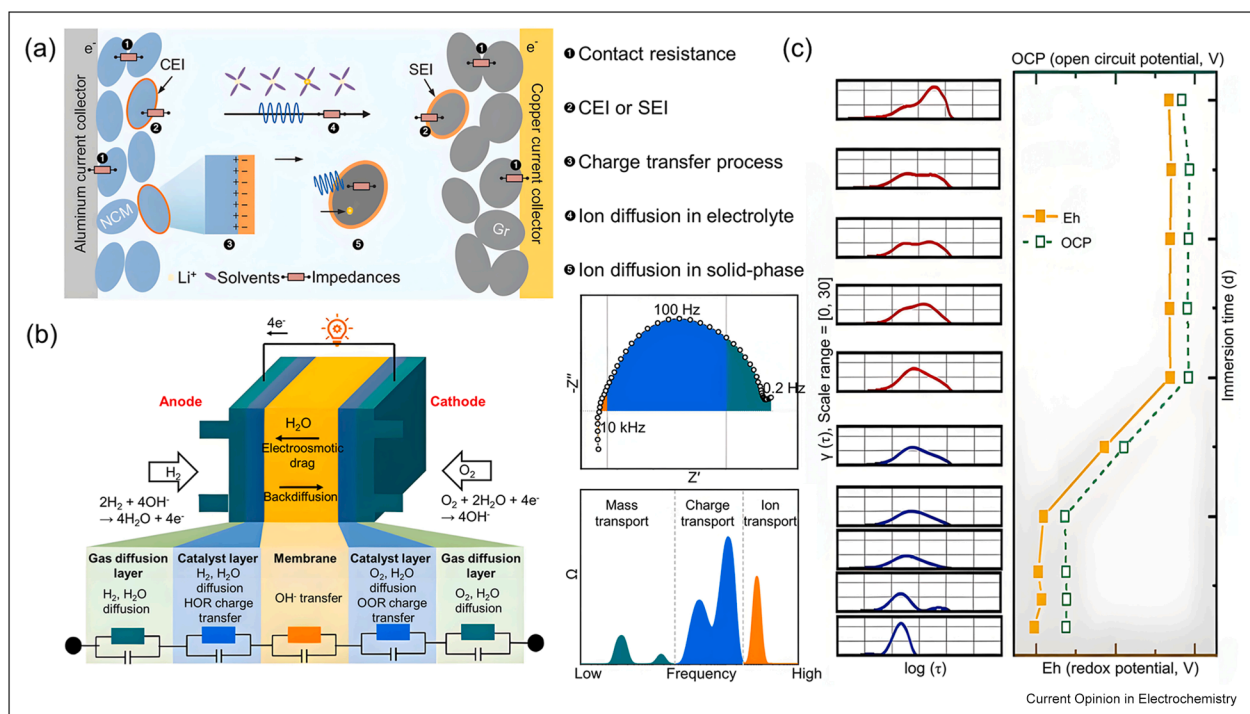
contributions. For example, in battery systems, solid electrolyte interphase (SEI)/cathode electrolyte interphase formation [21,22], charge transfer kinetics [5,23,24], solid-state diffusion [25,26], and mass transport limitations [27]. In rechargeable batteries, the evolution of the DRT spectrum over thousands of cycles can be tracked. It has been shown that the growth of a mid-frequency feature often correlates with SEI thickening [28,29], while a high-frequency shift to longer times has been attributed to loss of active material or degraded contact [30,31] (Figure 3(a)). Time-resolved DRT has clarified degradation in all-solid-state batteries by linking performance loss to interfacial dynamics at solid–solid contacts under operating conditions [32–34]. In fuel cells, DRT enables mechanistic diagnosis by mapping characteristic timescales to specific phenomena, such as catalyst-layer flooding (low-frequency, mass transport peaks) [35,36], membrane dehydration (increased high-frequency proton transport resistance) [37], and anode poisoning [38] (Figure 3(b)). For instance, in protonic ceramic fuel cells, DRT has been used to deconvolve air-electrode impedance into charge transfer,

ion migration, and surface exchange, thereby informing electrode design [39–41].

### DRT-informed predictive diagnostics

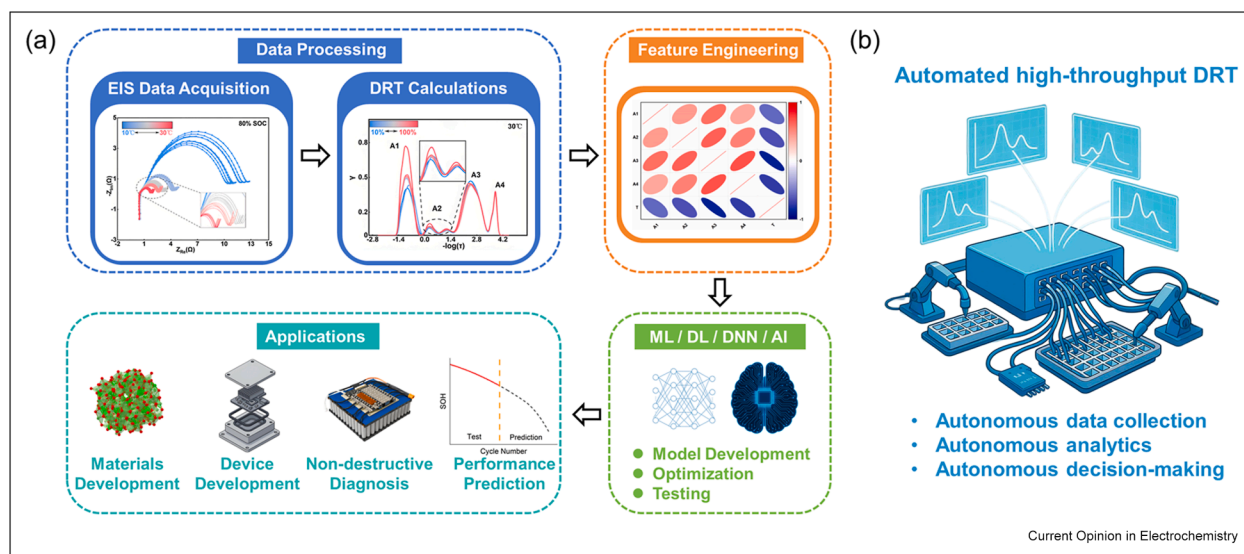
A notable trend is the use of DRT-derived features for predictive diagnostics [28,44,45]. Quantitative descriptors, including peak area, location, and width, serve as inputs to machine learning models for estimating state variables [46,47]. For example, Zhao *et al.* showed that incorporating DRT features in a hybrid model improved state-of-health (SOH) prediction relative to models based solely on raw impedance [46]. Because these descriptors are anchored to identifiable physical processes, shifts in peak time constants admit direct mechanistic interpretation, enabling early-stage anomaly detection, and improving remaining-useful-life forecasts. A longer-term objective is to integrate fast DRT algorithms with onboard battery management systems for real-time adaptive control and early warning, supporting digital-twin frameworks [48–51].

Figure 3



Application examples of DRT. **(a)** Mechanisms of timescale identifications of a typical Li-ion battery (Copyright 2024, Authors, Wiley, reproduced with permission) [42]. **(b)** The ion, charge, and mass transport processes are illustrated at their respective locations in the anion exchange membrane fuel cell (AEMFC) and corresponding DRT plot, divided into three regions, with ion, charge, and mass transport resistance (Copyright 2025, Authors, Wiley, reproduced with permission) [37]. **(c)** The corrosion evaluation of the aerobic–anaerobic corrosion transition of low-carbon steel under deep geological disposal conditions by DRT analysis. CEI, cathode electrolyte interphase; DRT, distribution of relaxation times; SEI, solid electrolyte interphase. (Copyright 2025, Elsevier, reproduced with permission) [43].

Figure 4



More technologies for DRT analysis. **(a)** The common workflow framework of developing machine learning/deep learning/deep neural network/artificial intelligence models for DRT analysis (Copyright 2025, Elsevier, reproduced with permission) [48]. **(b)** Schematic diagram for automated high-throughput DRT analysis. DRT, distribution of relaxation times; EIS, electrochemical impedance spectroscopy.

Extensions include internal temperature estimation and diagnosis of specific faults (e.g. lithium plating). A longer-term goal is to integrate fast DRT algorithms into battery-management systems to enable real-time adaptive control and early warning within digital-twin frameworks.

### Unraveling complexity in emerging electrochemical systems

Improved deconvolution reliability is also enabling studies in systems with partially understood physics. In corrosion science, DRT has yielded insights into passive-film evolution [52] and alloy corrosion mechanisms [53]; for example, Wang et al. identified the aerobic-to-anaerobic transition of steel under deep geological disposal by linking a specific DRT feature to oxygen depletion [43] (Figure 3(c)). In perovskite solar cells, a dual-DRT approach separated timescales associated with fast capacitive charging, trap-mediated recombination, and ionic migration [54,55]. Applications are also emerging in bioimpedance, where DRT can resolve continuous relaxations in cells and tissues more faithfully than classical Cole–Cole models [56] and in breast tumor monitoring by impedance tomography using Gaussian relaxation-time distributions [57]. More broadly, DRT has been applied to electrolyzers [58], photoelectrochemical synthesis [59], agricultural monitoring [60], gas sensing [61], electric capacitors [62], desalination [63], construction materials [64], and photocurrent spectroscopy [65]. This breadth underscores the need for rigor: validation against complementary measurements should accompany DRT analyses in nascent applications to avoid artifact-driven interpretation.

### Conclusions and perspectives

Progress on the ill-posed inverse problem has increased the reliability and utility of DRT. Methods that quantify uncertainty, suppress artifacts, and scale to large datasets have shifted DRT from qualitative interpretation to a quantitative, predictive framework.

A logical next step is multidimensional DRT, parameterizing processes over  $\ln \tau$  and covariates (SOH, SOC, temperature, and partial pressure). This facilitates cross-validation of peak assignments and process-level modeling. Substantial progress is likewise contingent upon standardization: the establishment of open-benchmark datasets that couple synthetic ground truth with curated measurements on canonical systems, as well as transparent reporting of code, hyperparameters, and raw data. Journals and agencies can accelerate progress by encouraging deposition of data and code and by adopting concise DRT-reporting checklists.

A pragmatic long-term objective is to integrate robust DRT into transparent, automated platforms. At the application level, models trained on high-throughput datasets that correlate experimental covariates with interpretable DRT features can facilitate precise SOH regression, mechanistic differentiation, and fault diagnosis (Figure 4(a)). These functionalities inspire the development of fully automated, closed-loop workflows capable of data acquisition, analysis with uncertainty quantification, and real-time adaptation of experimental conditions, thereby decreasing costs and enhancing reproducibility (Figure 4(b)). Transparent

implementations will expand accessibility and encourage proper usage. By emphasizing rigor, reproducibility, and judicious automation, the community can guarantee that DRT remains a dependable instrument for discovery and innovation within the field of electrochemistry.

### Declaration of Generative AI and AI-assisted technologies in the manuscript preparation process

During the preparation of this work the authors used Gemini (Google) in order to improve the language and clarity of certain parts. After using this tool/service, the authors reviewed and edited the content as needed and take full responsibility for the content of the published article.

### Declaration of competing interest

There are no competing interests to disclose.

### Acknowledgements

F.C. gratefully acknowledges the University of Bayreuth and the Bavarian Center for Battery Technology (BayBatt) for start-up funding. This work was partly funded by the Deutsche Forschungsgemeinschaft (DFG, German Research Foundation, 533115776). The authors thank the Research Grant Council of Hong Kong for support through the project 16201622. Y.W. acknowledges the support from the RGC Junior Research Fellow Scheme (JRF52526-6S08).

### List of abbreviations and symbols

EIS	Electrochemical impedance spectroscopy
DRT	Distribution of relaxation times
SOC	State of charge
SOH	State of health
SEI	Solid electrolyte interphase
CEI	Cathode electrolyte interphase
$\tau$	Timescale
$Z$	Impedance
$f$	Frequency
$\omega$	Angular frequency, $\omega = 2\pi f$
$\gamma(\log \tau)$	Distribution of relaxation times
$R_\infty$	Series resistance
$i$	Imaginary unit
$L_0$	Inductive component
$C_0$	Capacitive component
$\lambda$	Regularization parameter

### Data availability

No data was used for the research described in the article.

### References

Papers of particular interest, published within the period of review, have been highlighted as:

- \* of special interest
- \*\* of outstanding interest

- Vivier V, Orazem ME: **Impedance analysis of electrochemical systems**. *Chem Rev* 2022, **122**:11131–11168, <https://doi.org/10.1021/acs.chemrev.1c00876>.
- Macdonald DD: **Why electrochemical impedance spectroscopy is the ultimate tool in mechanistic analysis**. *ECS Trans* 2009, **19**:55, <https://doi.org/10.1149/1.3247566>.
- Maradesa A, Py B, Huang J, Lu Y, Lurilli P, Mrozinski A, *et al.*: **Advancing electrochemical impedance analysis through innovations in the distribution of relaxation times method**. *Joule* 2024, **8**:1958–1981, <https://doi.org/10.1016/j.joule.2024.05.008>.  
A significant community effort tracing the future of the DRT.
- Ivers T, Eacute EE, Weber A: **Eacute: Evaluation of electrochemical impedance spectra by the distribution of relaxation times**. *J Ceram Soc Jpn* 2017, **125**:193–201, <https://doi.org/10.2109/jcersj2.16267>.
- Chen J, Quattrocchi E, Ciucci F, Chen Y: **Charging processes in lithium-oxygen batteries unraveled through the lens of the distribution of relaxation times**. *Chem* 2023, **9**:2267–2281, <https://doi.org/10.1016/j.chempr.2023.04.022>.
- Wan TH, Saccoccio M, Chen C, Ciucci F: **Influence of the discretization methods on the distribution of relaxation times deconvolution: implementing radial basis functions with drttools**. *Electrochim Acta* 2015, **184**:483–499, <https://doi.org/10.1016/j.electacta.2015.09.097>.
- Wang Z, Wang Y, Py B, Maradesa A, Liu J, Wan TH, *et al.*: **Drttools: freely accessible distribution of relaxation times analysis for electrochemical impedance spectroscopy**. *ACS Electrochemistry* 2025, **1**, 12, 2680–2689, <https://doi.org/10.1021/acselectrochem.5c00334>.  
An open-source freely accessible online platform for DRT calculation and analysis.
- Fuoss RM, Kirkwood JG: **Electrical properties of solids. VIII. Dipole moments in polyvinyl chloride-diphenyl systems**. *J Am Chem Soc* 1941, **63**:385–394, <https://doi.org/10.1021/ja01847a013>.
- Keiter H, Rosenberg M: **On the probability distributions of relaxation times in glasses**. *Eur Phys J B* 1998, **5**:599–603, <https://doi.org/10.1007/s100510050484>.
- Chen J, Olver S: **Computing inverses of stieltjes transforms of probability measures**. *arXiv preprint arXiv:241016178* 2024. <https://doi.org/10.48550/arXiv.2410.16178>; 2024.
- Zhao Y, Kumtepelı V, Ludwig S, Jossen A: **Investigation of the distribution of relaxation times of a porous electrode using a physics-based impedance model**. *J Power Sources* 2022, **530**, 231250, <https://doi.org/10.1016/j.jpowsour.2022.231250>.
- Maradesa A, Py B, Quattrocchi E, Ciucci F: **The probabilistic deconvolution of the distribution of relaxation times with finite gaussian processes**. *Electrochim Acta* 2022, **413**, 140119, <https://doi.org/10.1016/j.electacta.2022.140119>.
- Williams NJ, Osborne C, Seymour ID, Bazant MZ, Skinner SJ: **Application of finite gaussian process distribution of relaxation times on soft electrodes**. *Electrochem Commun* 2023, **149**, 107458, <https://doi.org/10.1016/j.elecom.2023.107458>.
- Huang J, Sullivan NP, Zakutayev A, O'Hayre R: **How reliable is distribution of relaxation times (drt) analysis? A dual regression-classification perspective on drt estimation, interpretation, and accuracy**. *Electrochim Acta* 2023, **443**, 141879, <https://doi.org/10.1016/j.electacta.2023.141879>.

15. Bošković P, Žnidarič L, Gradišar Ž, Subotić V: **Probabilistic deconvolution for electrochemical impedance through variational bayesian inference.** *J Power Sources* 2024, **622**, 235359, <https://doi.org/10.1016/j.jpowsour.2024.235359>.
16. Huang J, Papac M, O'Hayre R: **Towards robust autonomous impedance spectroscopy analysis: a calibrated hierarchical bayesian approach for electrochemical impedance spectroscopy (eis) inversion.** *Electrochim Acta* 2021, **367**, 137493, <https://doi.org/10.1016/j.electacta.2020.137493>.
17. Ciucci F, Chen C: **Analysis of electrochemical impedance spectroscopy data using the distribution of relaxation times: a bayesian and hierarchical bayesian approach.** *Electrochim Acta* 2015, **167**:439–454, <https://doi.org/10.1016/j.electacta.2015.03.123>.
18. Py B, Wang Z, Wang Y, Ciucci F: **Entropy-based regularized regression for advanced distribution of relaxation times deconvolution.** *J Power Sources* 2025, **644**, 236910, <https://doi.org/10.1016/j.jpowsour.2025.236910>.
19. Liu J, Ciucci F: **Adaptive distribution of relaxation time analysis using bayesian mixtures.** 2025, <https://doi.org/10.26434/chemrxiv-2025-znq23>.
20. Quattrocchi E, Py B, Maradesa A, Meyer Q, Zhao C, Ciucci F: **Deconvolution of electrochemical impedance spectroscopy data using the deep-neural-network-enhanced distribution of relaxation times.** *Electrochim Acta* 2023, **439**, 141499, <https://doi.org/10.1016/j.electacta.2022.141499>.
21. Ma Z, Ruan D, Wang D, Lu Z, He Z, Guo J, et al.: **Selective methylation of cyclic ether towards highly elastic solid electrolyte interphase for silicon-based anodes.** *Angew Chem Int Ed* 2025, **64**, e202414859, <https://doi.org/10.1002/anie.202414859>.
22. Liu M, Yang K, Xie Q, Hu N, Zhang M, Chen R, et al.: **Operando evolution of a hybrid metallic alloy interphase for reversible aqueous zinc batteries.** *Angew Chem Int Ed* 2025, **64**, e202416047, <https://doi.org/10.1002/anie.202416047>.
23. Yao L, Liu J, Zhang F, Wen B, Chi X, Liu Y: **Reconstruction of zinc-metal battery solvation structures operating from  $-50 \sim +100$  °C.** *Nat Commun* 2024, **15**:6249, <https://doi.org/10.1038/s41467-024-50219-x>.
24. Wang Z: **Distribution of relaxation times for impedance analysis in batteries and fuel cells.** *Nat Rev Clean Technol* 2025, **1**, <https://doi.org/10.1038/s44359-025-00071-z>. 453-453.
25. Hu Z, Gao P, Ju S, Li Y, Zhang T, Lu C, et al.: **Dynamic volume compensation realizing ah-level all-solid-state silicon-sulfur batteries.** *Nat Commun* 2025, **16**:3979, <https://doi.org/10.1038/s41467-025-59224-0>.
26. Lee D, Shim Y, Kim Y, Kwon G, Choi SH, Kim K, et al.: **Shear force effect of the dry process on cathode contact coverage in all-solid-state batteries.** *Nat Commun* 2024, **15**:4763, <https://doi.org/10.1038/s41467-024-49183-3>.
27. Lu L, Kardjilov N, Meng X, Dong K, Xu Y, Wu Q, et al.: **Visualizing the dynamic wetting and redistribution of electrolyte in lean-electrolyte lithium-sulfur pouch cells via operando neutron imaging.** *Adv Energy Mater* 2025, e01324, <https://doi.org/10.1002/aenm.202501324>. n/a.
28. Guo J, Xu Y, Exner M, Huang X, Li Y, Liu Y, et al.: **Unravelling the mechanism of pulse current charging for enhancing the stability of commercial  $\text{LiNi}_{0.5}\text{Mn}_{0.3}\text{Co}_{0.2}\text{O}_2$ /graphite lithium-ion batteries.** *Adv Energy Mater* 2024, **14**, 2400190, <https://doi.org/10.1002/aenm.202400190>.
- DRT was applied to commercial NMC532/graphite 18,650 cells to reveal the key factors for the cycle life of commercial batteries.
29. Lin J, Hu W, Yang J, Pan L, Xia X, Wei Y, et al.: **Revisiting high-frequency impedance in li-ion batteries: decoupling solid electrolyte interphase resistance from pore impedance.** *J Phys Chem Lett* 2025, **16**:7490–7497, <https://doi.org/10.1021/acs.jpcllett.5c01426>.
30. Semerukhin DY, Kubarkov AV, Sergeyev VG, Semerukhin OA, Antipov EV: **Analysis of the distribution of relaxation times (drt) responses of li-ion cells as a function of their preparation conditions.** *Electrochim Acta* 2024, **486**, 144092, <https://doi.org/10.1016/j.electacta.2024.144092>.
31. Shao A, Wang H, Zhang M, Liu J, Cheng L, Li Y, et al.: **Multiscale interfacial stabilization via prelithiation separator engineering for ah-level anode-free lithium batteries.** *Nat Commun* 2025, **16**: 4145, <https://doi.org/10.1038/s41467-025-59521-8>.
32. Holmes SE, Zhang W, Kim SC, Cui Y: **A new lithium thioborate–lithium iodide solid-state electrolyte with high ionic conductivity for lithium metal batteries.** *ACS Energy Lett* 2024, **9**:1898–1906, <https://doi.org/10.1021/acscenergylett.4c00057>.
33. Li L, Deng L, Zhang K, Jiang R, Liu G, Li G, et al.: **Zr-doping induced complete amorphization toward highly stable all-solid-state sodium batteries.** *Adv Energy Mater* 2025, e03595, <https://doi.org/10.1002/aenm.202503595>. n/a.
34. Yu C-Y, Choi J, Dunham J, Ghahremani R, Liu K, Lindemann P, et al.: **Time-resolved impedance spectroscopy analysis of aging in sulfide-based all-solid-state battery full-cells using distribution of relaxation times technique.** *J Power Sources* 2024, **597**, 234116, <https://doi.org/10.1016/j.jpowsour.2024.234116>.
35. Jiang W, Ge C, Wang G, Lu J, Xiao L, Zhuang L: **Alleviating anode flooding by mesoporous carbon supports for alkaline polymer electrolyte fuel cells.** *Chin J Catal* 2024, **57**:51–58, [https://doi.org/10.1016/S1872-2067\(23\)64564-4](https://doi.org/10.1016/S1872-2067(23)64564-4).
36. Nasarre Artigas S, Xu H, Mack F: **Use of distribution of relaxation times analysis as an in-situ diagnostic tool for water management in pem fuel cells applications.** *J Power Sources* 2024, **600**, 234179, <https://doi.org/10.1016/j.jpowsour.2024.234179>.
37. Huang H, Zhang Z, Xiao C, Liu J, Li Z, Jiang Y, et al.: **Water management fault diagnosis by operando distribution of relaxation times analysis for anion exchange membrane fuel cells.** *Adv Sci* 2025, **12**, 2505304, <https://doi.org/10.1002/advs.202505304>.
38. Li W, Wang Q, Liu Y, Wu L, Pan Z, Chen R, et al.: **Unravelling degradation mechanisms of anion exchange membrane direct ammonia fuel cells via distribution of relaxation times.** *Chem Eng J* 2025, **512**, 162204, <https://doi.org/10.1016/j.cej.2025.162204>.
39. Błaszczak P, Mäkinen P, Mroziński A, Ducka A, Jasiński G, Himanen O, et al.: **Uncovering the electrochemical processes and understanding the causes of the degradation via eis-drt in large-scale solid oxide fuel cell.** *Appl Energy* 2025, **393**, 125983, <https://doi.org/10.1016/j.apenergy.2025.125983>.
- In-situ EIS-DRT “electrochemical fingerprint” was established for fuel cell to diagnose operating degradation.
40. Han Z, Dong H, Wang Y, Yang Y, Yu H, Yang Z: **Mechanistic insight into catalytic conversion of methane on a  $\text{Sr}_{2}\text{Fe}_{1.5}\text{Mo}_{0.5}\text{O}_{6-\delta}$  perovskite anode: a combined eis-drt, dft and tpsr investigation.** *J Mater Chem A* 2023, **11**:18820–18831, <https://doi.org/10.1039/D3TA03391K>.
41. Liang M, Wang Y, Song Y, Guan D, Wu J, Chen P, et al.: **High-temperature water oxidation activity of a perovskite-based nanocomposite towards application as air electrode in reversible protonic ceramic cells.** *Appl Catal B Environ* 2023, **331**, 122682, <https://doi.org/10.1016/j.apcatb.2023.122682>.
42. Cai X, Zhang C, Ruan H, Chen Z, Zhang L, Sauer DU, et al.: **Cross-scale decoupling kinetic processes in lithium-ion batteries using the multi-dimensional distribution of relaxation time.** *Adv Sci* 2024, **11**, 2406934, <https://doi.org/10.1002/advs.202406934>.
43. Wang Y, Qiao S, Xie J, Wang Y, Hao L, Wang J, et al.: **Drt analysis on eis data to identify aerobic-anaerobic corrosion evolution of low-carbon steel under deep geological disposal condition.** *Corros Sci* 2025, **255**, 113118, <https://doi.org/10.1016/j.corsci.2025.113118>.
- DRT was employed combined with redox potential monitoring for the aerobic-anaerobic corrosion transition investigation of low-carbon steel.
44. Huang JD, Meisel C, Sullivan NP, Zakutayev A, O'Hayre R: **Rapid mapping of electrochemical processes in energy-conversion devices.** *Joule* 2024, **8**:2049–2072, <https://doi.org/10.1016/j.joule.2024.05.003>.

45. Wu Y-W, Li C-C: **Electrochemical assessment of a li-ion full cell with cathode-anode impedance separation via in-situ eis-drt and three-electrode configuration.** *J Power Sources* 2025, **630**, 236115, <https://doi.org/10.1016/j.jpowsour.2024.236115>.
46. Zhao X, Liu S, Li E, Wang Z, Gu F, Ball AD: **A hybrid intelligent model using the distribution of relaxation time analysis of electrochemical impedance spectroscopy for lithium-ion battery state of health estimation.** *J Energy Storage* 2024, **84**, 110814, <https://doi.org/10.1016/j.est.2024.110814>.  
Using DRT data with neural networks to build a SOH evaluation model, delivering temperature-robust, higher-accuracy SOH estimation than raw-EIS features or standard models.
47. Zhang L, Hong X, Xu W, Ruan D: **Research on estimating the state of health of power batteries based on the distribution of relaxation times method.** *J Energy Storage* 2024, **94**, 112370, <https://doi.org/10.1016/j.est.2024.112370>.
48. Chen X, Li Q, Shao B, Dou W, Lai C, Lu T, *et al.*: **Accurately estimating internal temperature of lithium-ion batteries based on the distribution of relaxation time and data-driven.** *Energy* 2025, **320**, 135493, <https://doi.org/10.1016/j.energy.2025.135493>.
49. Jung MJ, Lee S-G, Choi K-S: **A new diagnostic indicator for lithium-ion batteries via electrochemical impedance spectroscopy: harnessing the highest frequency peak in distribution of relaxation times.** *J Power Sources* 2024, **611**, 234743, <https://doi.org/10.1016/j.jpowsour.2024.234743>.
50. Wang F, Liu S, Chen S, Zhang Q, Wang D, Ma X, *et al.*: **SoH estimation for lithium-ion batteries using distribution of relaxation time and feature optimized multilayer perceptron.** *iScience* 2025, 113443, <https://doi.org/10.1016/j.isci.2025.113443>.
51. Py B, Ciucci F: **Fast fourier transform-based distribution of relaxation times analysis for efficient and flexible time-domain electrochemical impedance characterization.** *J Electrochem Soc* 2025, **172**, 026504, <https://doi.org/10.1149/1945-7111/adb33f>.  
A novel methodology for simultaneous recovery of impedance and DRT from voltage responses to arbitrary current excitation under a DRT constraint.
52. Figueroa R, Díaz B, Nóvoa XR, Pérez C: **Corrosion protection of carbon steel by water-borne resin modified by reduced-graphene oxide.** *Prog Org Coating* 2025, **201**, 109148, <https://doi.org/10.1016/j.porgcoat.2025.109148>.
53. Prabhakaran V, Strange L, Kalsar R, Marina OA, Upadhyay P, Joshi VV: **Investigating electrochemical corrosion at mg alloy-steel joint interface using scanning electrochemical cell impedance microscopy (seccim).** *Sci Rep* 2023, **13**, 13250, <https://doi.org/10.1038/s41598-023-39961-2>.
54. Hernández-Balaguera E, Romero B, Najafi M, Galagan Y: **Analysis of light-enhanced capacitance dispersion in perovskite solar cells.** *Adv Mater Interfac* 2022, **9**, 2102275, <https://doi.org/10.1002/admi.202102275>.
55. Patel RD, Chaudhary KJ, Purohit D, Prochowicz D, Akin S, Kalam A, *et al.*: **Dual drt-based deconvolution of electrochemical signatures in perovskite solar cells.** *J Energy Chem* 2025, **109**: 975–984, <https://doi.org/10.1016/j.jechem.2025.05.056>.
56. Ramírez-Chavarría RG, Sánchez-Pérez C, Matatagui D, Qureshi N, Pérez-García A, Hernández-Ruiz J: **Ex-vivo biological tissue differentiation by the distribution of relaxation times method applied to electrical impedance spectroscopy.** *Electrochim Acta* 2018, **276**:214–222, <https://doi.org/10.1016/j.electacta.2018.04.167>.
57. Setyawan G, Sejati PA, Ibrahim KA, Takei M: **Breast cancer recognition by electrical impedance tomography implemented with gaussian relaxation-time distribution (eit-grtd).** *J Electri Bioimpedance* 2024, **15**:99–106, <https://doi.org/10.2478/joeb-2024-0011>.
58. Sun Y, Bai F, Liu J, Sun S, Mao Y, Liu X, *et al.*: **Identification of degradation reasons for a co2 mea electrolyzer using the distribution of relaxation times analysis.** *J Phys Chem Lett* 2024, **15**: 9122–9128, <https://doi.org/10.1021/acs.jpcclett.4c02024>.
59. Li D, Wei R, Zhang D, Ni C, Yin H, Zhang L, *et al.*: **Determining kinetics of h2o2 evolution from photoelectrochemical water oxidation.** *Nat Commun* 2025, **16**:7875, <https://doi.org/10.1038/s41467-025-62828-1>.
60. Van Haeverbeke M, De Baets B, Stock M: **Evaluating the potential of distribution of relaxation times analysis for plant agriculture.** *Comput Electron Agric* 2023, **213**, 108249, <https://doi.org/10.1016/j.compag.2023.108249>.
61. Deng Z, Yang A, Wan X, Chu J, Pan J, Wang Q, *et al.*: **Discrimination and prediction of sf6 decomposition gas mixtures based on distribution of relaxation time analysis.** *Microchem J* 2025, **217**, 114871, <https://doi.org/10.1016/j.microc.2025.114871>.
62. Li Z, Feng H, Jia B, Zuo Z, Mei B-A: **Identification of thermal process of electric double layer capacitor systems by distribution of relaxation times analysis for thermal impedance spectroscopy.** *J Energy Storage* 2023, **64**, 107152, <https://doi.org/10.1016/j.est.2023.107152>.
63. Kim N, Park J, Cho Y, Yoo C-Y: **Comprehensive electrochemical impedance spectroscopy study of flow-electrode capacitive deionization cells.** *Environ Sci Technol* 2023, **57**: 8808–8817, <https://doi.org/10.1021/acs.est.3c01619>.
64. Harirchi P, Yang M: **Effect of carbon dioxide curing on cement pastes through drt analysis of eis data.** *Constr Build Mater* 2024, **417**, 135310, <https://doi.org/10.1016/j.conbuildmat.2024.135310>.
65. Piccioni A, Vecchi P, Vecchi L, Grandi S, Caramori S, Mazzaro R, *et al.*: **Distribution of relaxation times based on lasso regression: a tool for high-resolution analysis of imps data in photoelectrochemical systems.** *J Phys Chem C* 2023, **127**: 7957–7964, <https://doi.org/10.1021/acs.jpcc.3c00770>.